

Neutrino imaging of the Galactic Centre and Millisecond Pulsar Population

Paul C. W. Lai,^{a,*} Matteo Agostini,^b Foteini Oikonomou,^c Beatrice Crudele,^b Ellis R. Owen^d and Kinwah Wu^a

^aMullard Space Science Laboratory, University College London,
Holmbury St. Mary, Surrey RH5 6NT, United Kingdom

^bDepartment of Physics and Astronomy, University College London,
Gower Street, London, WC1E 6BT, United Kingdom

^cInstitutt for Fysikk, Norwegian University of Science and Technology,
Trondheim, Norway

^dTheoretical Astrophysics, Department of Earth and Space Science, Graduate School of Science,
Osaka University, Toyonaka, Osaka 560-0043, Japan

E-mail: chong.lai.22@ucl.ac.uk

Despite the potentially large population of millisecond pulsars in the Galactic Centre, direct detection of them is almost impossible using the current radio telescopes, due to severe pulse broadening caused by radiation scattering. We propose that imaging the Galactic Centre using neutrinos provides us a way to constrain the millisecond pulsar population. Millisecond pulsars are proposed cosmic-ray accelerators. The high-energy protons they produce will collide with the baryonic matter in the central molecular zone, which creates charged and neutral pions that decay into neutrinos and γ rays, respectively. The specific fluxes of neutrino and γ -ray emission for the case with CS emission as the baryon tracer in the Central Molecular Zone that we computed, subjected to γ -ray observation by H.E.S.S., set a conservative upper limit of $N_{\text{MSP}} < 10,000$ for the Galactic Centre millisecond pulsar population, with a injecting proton energy spectral index $\Gamma = -1$ and an efficiency of $f_p = 1\%$ converting the pulsar's rotational power to cosmic-ray power. This population of millisecond pulsars could explain the GeV γ -ray excess in the Galactic Centre.

38th International Cosmic Ray Conference (ICRC2023)
26 July - 3 August, 2023
Nagoya, Japan



*Speaker

1. Overview

It has been suggested the Galactic Centre (GC) harbours a large number of pulsars [see 1, 2]. Verifying the presence or absence of these pulsars could help to resolve issues such as the origin(s) of the strong γ -rays, and the stellar-mass black-hole content in the GC region. The fast rotation, together with a strong magnetic field, of a pulsar creates a large electric potential difference between the pulsar polar cap to the equator, and this electric potential gap accelerates charged particles to high energies [3]. Pulsars, and in particular millisecond pulsars (MSPs), are therefore expected to be cosmic-ray (CR) sources [see e.g. 4].

The TeV γ -ray emission observed in the GC region implies the presence of localised PeV accelerators, if the γ -rays are by-products of CR interactions [see 5, 6]. The massive nuclear black hole (Sgr A*), supernova remnants, star clusters and pulsars are candidate PeV charged-particle accelerators. Sgr A* has been inactive since about 1 Myr ago [7, 8]. The PeV CRs it could have produced would have diffused away from the GC region by now. In fact, H.E.S.S. observations indicate that the injection of PeV CRs at the GC is more likely to be continuous rather than episodic [5]. Extreme supernova remnants could produce PeV CRs [9], but such extreme supernovae are uncommon. The two remaining candidates are therefore the nuclear star cluster and pulsars, in particular MSPs [3, 10]. In this work, we focus on the latter, the pulsars.

Direct detection of GC pulsars, including MSPs, through traditional timing radio observations, is difficult, because of severe pulse broadening caused by scattering due to the ionised gas. Alternative means must be sought for identifying this pulsar population, if present. We investigate the possible non-photonic signatures aiming to gain insights into the GeV γ -ray excess and the missing pulsar problem [see e.g. 2, 11]. Accepting that MSPs are CR sources, there should be observational signatures of their CRs distinguishable from those belonging to the background CRs [see e.g. see the neutrino image of the Galactic Plane generated from IceCube observations, 12], which are known to be present in Galactic Plane. We argue that the CRs from GC MSPs would interact with the diffuse media in their vicinity, through hadronic p-p processes. The decays of the produced charged pions from the p-p interactions will give rise to high-energy neutrinos. The Central Molecular Zone (CMZ) [see e.g. 13] provides the target baryons for the hadronic interactions of the MSP CRs. As a consequence, the GC region will glow in high-energy neutrinos, tracking the locations of the dense media in the CMZ, which are detectable in future high spatial resolution neutrino imaging observations. These observations will verify the presence or the absence of the MSP population, and hence constrain the total number of GC MSPs.

2. Model Scenario

The studied scenario can be summarised as follows. Around Sgr A* there is a population of MSPs with a 1D radial distribution profile. Protons accelerated by the MSPs are scattered around by the interstellar magnetic field. Collocated with the MSPs in the GC is a spatially extended diffuse baryonic medium and most of the baryons are locked in the CMZ clouds. The GC CRs interact with these baryons in the CMZ, via p-p processes, which lead to pion cascades. Neutrinos are produced in the weak decays of charged pions π^\pm and γ -rays are emitted in electromagnetic decays of neutral pions π^0 .

2.1 Millisecond pulsars as particle accelerators

For a MSP with a rotational period P_s and polar strength B for a dipolar magnetic field, the spin-down luminosity

$$L_{\text{sd}} = 1.4 \times 10^{35} \text{ erg s}^{-1} \left(\frac{B}{10^8 \text{ G}} \right)^2 \left(\frac{R_{\text{ns}}}{10 \text{ km}} \right)^6 \left(\frac{P_s}{1 \text{ ms}} \right)^{-4}, \quad (1)$$

[14], where R_{ns} is the MSP (neutron star) radius. The maximum energy attained by the protons is

$$E_{\text{p,max}} = 2\eta \text{ PeV} \left(\frac{B}{10^8 \text{ G}} \right) \left(\frac{R_{\text{ns}}}{10 \text{ km}} \right)^2 \left(\frac{P_s}{1 \text{ ms}} \right)^{-1}. \quad (2)$$

As only a fraction of the rotational power of a MSP is used for accelerating the charged particles, a scaling parameter f_p is introduced. This gives the effective CR power

$$f_p L_{\text{sd}} = \int_{m_p c^2}^{\infty} dE_p Q_{\text{psr}}(E_p) E_p \propto \int_{m_p c^2}^{\infty} dE_p E_p^{\Gamma+1} e^{-E_p/E_{\text{p,max}}}, \quad (3)$$

of a MSP, where $Q_{\text{psr}}(E_p)$ is the spectral power, in the unit of $(\text{erg s})^{-1}$, and Γ is spectral index, of the CR protons produced by the MSP, and m_p is proton mass. The high-energy cut-off is set by $E_{\text{p,max}}$ (see Equation 2), and for a fixed f_p two MSPs could have the same spin-down luminosity, and hence the same CR power, yet different spectral cutoffs of their CR protons.

2.2 Cosmic-ray transport with hadronic interactions

The transport of CR protons in energy space is described by the diffusion equation, characterised by an energy-dependent diffusion coefficient, $D(E_p)$:

$$\frac{\partial n_p(E_p, r, t)}{\partial t} - \nabla \cdot [D(E_p) \nabla n_p(E_p, r)] = Q_{\text{psr}}(E_p) n_{\text{MSP}}(r) - c [n_{\text{H}} \sigma_{\text{pp}}(E_p)] n_p(E_p, r, t), \quad (4)$$

where n_p is the CR proton number density, n_{H} is the hydrogen number density in the diffuse medium, and n_{MSP} is the MSP number density in the GC region. The two terms on the right side of the equation are the rates of particle loss (through inelastic hadronic p-p interaction with cross section σ_{pp}) and of production of CR protons by MSPs. The general solution to the transport equation is

$$n_p(E_p, r) \approx \frac{Q_{\text{psr}}(E_p)}{4\pi D(E_p)} \int_r^{\infty} dr' \frac{N_{\text{MSP}}(r')}{r'^2}, \quad (5)$$

for $n_{\text{MSP}}(r)$, in the limits $r \ll 2\sqrt{Dt}$ (stationary limit) and $r \ll \sqrt{D/(cn_{\text{H}}\sigma_{\text{pp}})}$ (negligible absorption), with the number of pulsars within a radius r' given by $N_{\text{MSP}}(r') = \int_0^{r'} dr n_{\text{MSP}}(r) 4\pi r^2$. The all-favour neutrino and γ -ray fluxes are given by

$$\frac{dN_{\nu/\gamma}}{dE_{\nu/\gamma}} = \frac{1}{4\pi d^2} \int dV \frac{d\dot{n}_{\nu/\gamma}(E_{\nu/\gamma})}{dE_{\nu/\gamma}} \quad (6)$$

(observed at Earth), where

$$\frac{d\dot{n}_{\nu/\gamma}(E_{\nu/\gamma})}{dE_{\nu/\gamma}} = c n_{\text{H}} \int_{m_p}^{\infty} \frac{dE_p}{E_p} F_{\nu/\gamma} \left(\frac{E_{\nu/\gamma}}{E_p}, E_p \right) \sigma_{\text{pp}}(E_p) n_p(E_p, r). \quad (7)$$

Here, $F_{\nu/\gamma}$ is the transferred spectral function of the secondary neutrinos and γ rays in a single collision, and we have obtained it from [15, 16].

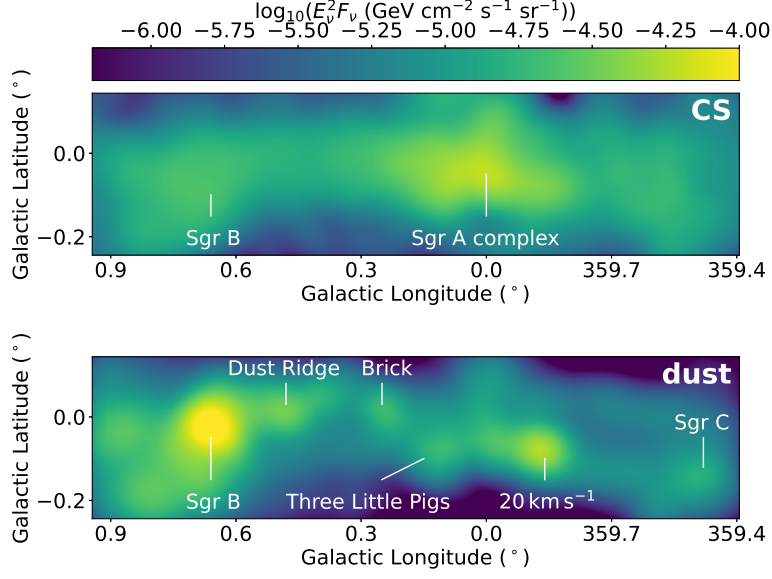


Figure 1: All-flavor neutrino surface brightness images at $E_\nu = 100$ TeV for $\Gamma = -1$ and $N_{\text{MSP}} = 5 \times 10^3 f_{p,1}^{-1}$. The effective angular resolution is 0.077° , same as the angular resolution of the CS observation [17]. The panels show the results for CS and dust emission as the mass tracer. Some of the known MCs are marked. More CMZ MCs can be found in [19, 20].

2.3 Central Molecular Zone

The observed neutrino and γ -ray fluxes are linearly dependent on the number density of the target baryon (hydrogen) (see Equation 7), which are predominantly in the CMZ. Ideally, we would use a 3D number density profile, but it is not directly observable. Instead, we use a line-of-sight hydrogen column density, which can be derived from IR or radio observations, to compute a sky map of neutrino and γ -ray intensities. The rationale behind this is that both neutrinos and γ -ray would not suffer attenuation propagating from the GC region to reach the Earth. CS (carbon monosulfide) and dust emission is often used as mass tracers for molecular clouds, but they give substantially different baryon distribution profiles in the CMZ [cf. 17, 18]. We therefore consider both CS and dust observations, taken from [17] and [18], respectively, to derive the hydrogen column density maps. The region within 359.4° to 0.95° in Galactic longitude and -0.25° to $+0.15^\circ$ in Galactic latitude, which sufficiently covers the densest structure of CMZ, and integration over the region yield a total mass of $\sim 7 \times 10^7 M_\odot$.

3. Results and discussion

We adopt a distance of $d = 8.28$ kpc from Earth to the GC [21] and a diffusion coefficient $D(E_p) = 2.24 \times 10^{28} \text{ cm}^2 \text{ s}^{-1} (E_p/1 \text{ GeV})^\alpha$ [22], where $\alpha = 0.21$ for the transport of CRs near the GC. Two groups of MSPs, with $(B, R_{\text{ns}}, P_s) = (10^8 \text{ G}, 10 \text{ km}, 1 \text{ ms})$ and $(B, R_{\text{ns}}, P_s) = (10^{10} \text{ G}, 10 \text{ km}, 10 \text{ ms})$, are considered in the calculations. They have the same spin-down luminosity but different maximum accelerated proton energy. The energy spectral indices of the CR protons that they produce are $\Gamma = -1, -1.5$ and -2 .

Figure 1 shows the all-flavour neutrino surface brightness images at $E_\nu = 100$ TeV for the case with number of GC MSPs $N_{\text{MSP}} = 5 \times 10^3 f_{\text{p},1}^{-1}$, and MSP CR energy spectral index $\Gamma = -1$. In generating the neutrino surface brightness images, we have considered also other choices of CR spectral properties, and we have found that the choices of Γ and E_ν would not alter the presence or absence of the bright features, which correspond to the region with a high concentration of baryons. It would however change the brightness normalisation, implying there is a degeneracy of the MSP CR spectra parameters, MSP number density, and the efficiency of converting the MSPs' rotational energy to CR luminosity. The effective angular resolution of the images is 0.077° . This image hints that the features shown in the two panels could be resolved at a spatial resolution of about 0.2° , or even 0.3° , which would be achievable in the new observatories located in the north hemisphere, such as KM3NeT, Baikal-GVD and P-ONE.

By inspecting and comparing the two panels in Figure 1 we may draw two qualitative conclusions. First, modelling using the baryon column density (hence, concentration) derived from CS emission and tracer from dust emission gives different features in the neutrino surface brightness map. A direct consequence of this is that CRs produced by the MSP in the GC regions are baryon "torches", and neutrino imaging can be used as a means to assess the reliability of different emissions as mass tracers of MCs in the GC region. Second, integrating the surface brightness over the image gives the emission power of neutrinos and hence a constraint on the power of the CRs that have produced them. This gives us some hints on the energy spectral properties of the MSP CRs, specific by Γ and $E_{\text{p,max}}$, the number density of MSPs M_{MSP} and the efficiency MSPs to produce CRs (f_{p}). A strong constraint cannot be drawn because of the degeneracy in these parameters and the convolution between some of them.

Figure 2 shows the spectra of the total all-flavor neutrino and γ -ray emission from the entire CMZ. In the calculations, the pulsars are located within $R = 20$ pc from the GC, and the baryon distribution in the CMZ is derived from the CS emission data [17]. The upper panels show how the spectra change with Γ by fixing the normalisation $f_{\text{p}}N_{\text{MSP}}$. We then adjust the population N_{MSP} to match the H.E.S.S. observation [6], which is shown in the lower panels of Figure 2. The γ -ray flux derived from our models should not exceed the H.E.S.S. observation [6], which constrains the possible population of MSPs. For example, for the $\Gamma = -1$ model, we can obtain a conservative upper limit of $N_{\text{MSP}} < 10,000$, assuming that $f_{\text{p}} = 1\%$. In all the models considered, the all-flavour neutrino specific flux tracks closely the γ -ray specific flux. Similar brightness features are therefore expected to be present in the neutrino and γ -ray surface brightness maps if there is no leptonic γ -ray emission. This implies that spectral imaging neutrino observations would allow us to probe the properties of the CR accelerators and constrain their number, and here the candidate accelerators are GC MSPs.

4. Conclusion

We consider MSPs as particle accelerators whose CRs interact with the baryons in the CMZ of the GC through hadronic processes. We calculate the neutrino and gamma-ray emissions resulting from these hadronic processes. We show the neutrino images of the GC with CS and dust emission as tracers of target baryons in the CMZ and demonstrate that neutrino imaging could be used to determine the baryon distribution in the GC. We compute the specific fluxes of neutrino and γ -ray

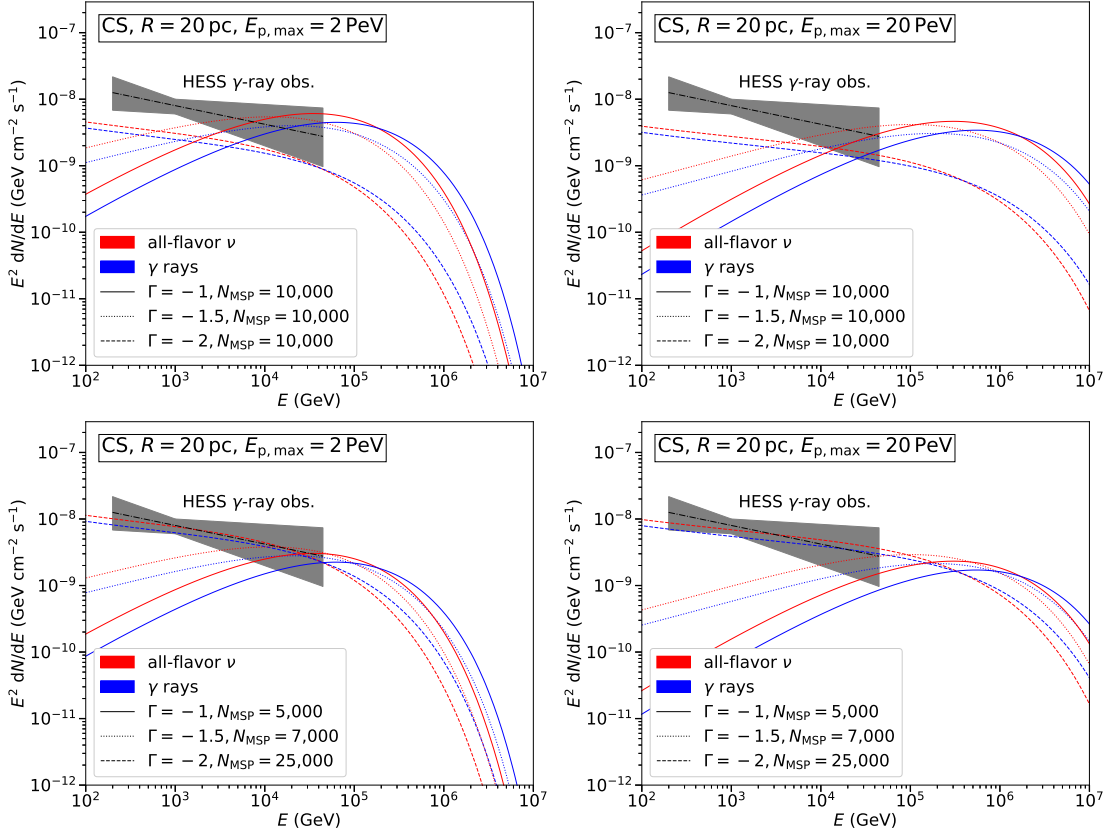


Figure 2: The computed spectra of total all-flavor neutrino and γ -ray emission from the entire CMZ with $R = 20$ pc, with CS emission as the baryon tracer. The spectrum of the γ -ray from GC detected by H.E.S.S. [6] is also shown, as dotted dash line, with the uncertainty represented by the grey band. In the upper panels, N_{MSP} is the same for all the models. In the lower panels, the normalisation for (N_{MSP}) is chosen such that the computed γ -ray specific flux matches that derived from the the H.E.S.S. observation. The acceleration efficiency f_p is set to be 1% for all calculations.

emission for the case with CS emission as the baryon tracer subjected to the limits set by the H.E.S.S. observations. We obtain a conservative upper limit of $N_{\text{MSP}} < 10,000$ for the GC MSP population, with CR energy spectral index $\Gamma = -1$ and efficiency of $f_p = 1\%$ converting the pulsar's rotational power to CR power. This limit varies with the model parameters, and it is inversely proportional to f_p . The sizes of MSP populations that we obtain are consistent with those required to explain the GeV γ -ray excess in GC. The results obtained in this work are benchmarks for future neutrino detectors that will observe the GC with high angular resolution ($< 1^\circ$).

Acknowledgments

PCWL is supported by the UCL Graduate Research Scholarship and Overseas Research Scholarship. PCWL, MA, BC and KW are supported by the UCL Cosmoparticle Initiative. ERO is an overseas researcher under the Postdoctoral Fellowship of the Japan Society for the Promotion of Science (JSPS), supported by JSPS KAKENHI Grant Number JP22F22327.

References

- [1] E. Pfahl and A. Loeb, *Probing the Spacetime around Sagittarius A* with Radio Pulsars*, *ApJ* **615** (2004) 253 [[astro-ph/0309744](#)].
- [2] R.S. Wharton, S. Chatterjee, J.M. Cordes, J.S. Deneva and T.J.W. Lazio, *Multiwavelength Constraints on Pulsar Populations in the Galactic Center*, *ApJ* **753** (2012) 108 [[1111.4216](#)].
- [3] C. Guépin, B. Cerutti and K. Kotera, *Proton acceleration in pulsar magnetospheres*, *A&A* **635** (2020) A138 [[1910.11387](#)].
- [4] K. Kotera and A.V. Olinto, *The Astrophysics of Ultrahigh-Energy Cosmic Rays*, *ARA&A* **49** (2011) 119 [[1101.4256](#)].
- [5] H.E.S.S. Collaboration, A. Abramowski, F. Aharonian, F.A. Benkhali, A.G. Akhperjanian, E.O. Angüner et al., *Acceleration of petaelectronvolt protons in the Galactic Centre*, *Nature* **531** (2016) 476 [[1603.07730](#)].
- [6] H. E. S. S. Collaboration, H. Abdalla, A. Abramowski, F. Aharonian, F. Ait Benkhali, A.G. Akhperjanian et al., *Characterising the VHE diffuse emission in the central 200 parsecs of our Galaxy with H.E.S.S.*, *A&A* **612** (2018) A9 [[1706.04535](#)].
- [7] F. Guo and W.G. Mathews, *The Fermi Bubbles. I. Possible Evidence for Recent AGN Jet Activity in the Galaxy*, *ApJ* **756** (2012) 181 [[1103.0055](#)].
- [8] H.Y.K. Yang, M. Ruszkowski and E.G. Zweibel, *Fermi and eROSITA bubbles as relics of the past activity of the Galaxy's central black hole*, *Nature Astronomy* **6** (2022) 584.
- [9] A. Marcowith, V.V. Dwarkadas, M. Renaud, V. Tatischeff and G. Giacinti, *Core-collapse supernovae as cosmic ray sources*, *MNRAS* **479** (2018) 4470 [[1806.09700](#)].
- [10] G. Morlino, P. Blasi, E. Peretti and P. Cristofari, *Particle acceleration in winds of star clusters*, *MNRAS* **504** (2021) 6096 [[2102.09217](#)].
- [11] R. Bartels, S. Krishnamurthy and C. Weniger, *Strong Support for the Millisecond Pulsar Origin of the Galactic Center GeV Excess*, *Phys. Rev. Lett.* **116** (2016) 051102.
- [12] IceCube Collaboration, *Observation of high-energy neutrinos from the Galactic plane*, *Science* **380** (2023) eaat1338.
- [13] E.A.C. Mills, *The Milky Way's Central Molecular Zone*, *arXiv e-prints* (2017) [arXiv:1705.05332](#) [[1705.05332](#)].
- [14] C. Guépin, L. Rinchuso, K. Kotera, E. Moulin, T. Pierog and J. Silk, *Pevatron at the Galactic Center: multi-wavelength signatures from millisecond pulsars*, *J. Cosmology Astropart. Phys.* **2018** (2018) 042 [[1806.03307](#)].
- [15] M. Kachelrieß, I.V. Moskalenko and S. Ostapchenko, *AAfrag: Interpolation routines for Monte Carlo results on secondary production in proton-proton, proton-nucleus and nucleus-nucleus interactions*, *Computer Physics Communications* **245** (2019) 106846.

- [16] S. Koldobskiy, M. Kachelrieß, A. Lskavyan, A. Neronov, S. Ostapchenko and D.V. Semikoz, *Energy spectra of secondaries in proton-proton interactions*, *Phys. Rev. D* **104** (2021) 123027 [2110.00496].
- [17] M. Tsuboi, T. Handa and N. Ukita, *Dense Molecular Clouds in the Galactic Center Region. I. Observations and Data*, *ApJS* **120** (1999) 1.
- [18] S. Molinari, J. Bally, A. Noriega-Crespo, M. Compiègne, J.P. Bernard, D. Paradis et al., *A 100 pc Elliptical and Twisted Ring of Cold and Dense Molecular Clouds Revealed by Herschel Around the Galactic Center*, *ApJ* **735** (2011) L33 [1105.5486].
- [19] M. Tsuboi, K.-I. Tadaki, A. Miyazaki and T. Handa, *Sagittarius A Molecular Cloud Complex in $H^{13}CO^+$ and Thermal SiO Emission Lines*, *PASJ* **63** (2011) 763.
- [20] C. Battersby, E. Keto, D. Walker, A. Barnes, D. Callanan, A. Ginsburg et al., *CMZoom: Survey Overview and First Data Release*, *ApJS* **249** (2020) 35 [2007.05023].
- [21] GRAVITY Collaboration, R. Abuter, A. Amorim, M. Bauböck, J.P. Berger, H. Bonnet et al., *Improved GRAVITY astrometric accuracy from modeling optical aberrations*, *A&A* **647** (2021) A59 [2101.12098].
- [22] D. Gaggero, A. Urbano, M. Valli and P. Ullio, *Gamma-ray sky points to radial gradients in cosmic-ray transport*, *Phys. Rev. D* **91** (2015) 083012 [1411.7623].